

## Nuclear Instrumentation: Lecture 3

## Pulse Processing: Preamplifiers and Noise

### 3.1 LINEAR AND LOGIC PULSES

In any application it is important to distinguish between two types of pulse trains. A *linear* pulse carries information through its amplitude and sometimes its shape (pulse shape discrimination for neutron and charged-particle measurement). A *logic* pulse is a pulse of a standard size or shape, which carries information only by its presence or absence or by its time of arrival. Virtually all detector signal chains start with a linear pulse train, which may subsequently be processed into logic pulses

#### 3.1.1 Linear pulses

Linear pulses can often be subdivided into:

- *Fast linear pulses:* Such as those produced by a fast, linear (timing-filter) amplifier (tfa). These usually have poor signal-to-noise properties. However, their rapid rise and fall times make them useful when extracting time information or when high counting rates are important.
- *Linear tail pulses:* Such as those produced by preamplifiers. These pulses may have reasonably rapid rise times but have a long decay time (typically 50 - 100  $\mu$ s). The rise time is determined by the charge collection time in the detector while the decay time is determined by the time constant of the shaping circuit. The pulse amplitude accurately reflects the energy deposited in the detector. Amplitude and the rise time of the leading edge are the important characteristics of linear tail pulses.
- *Shaped linear pulses:* These are produced by a linear amplifier. A shaped linear pulse is a tail pulse whose width has been dramatically reduced (to a few  $\mu$ s) by one or other of the shaping methods discussed previously.

### 3.1.2 Logic pulses

Two main classes of *logic pulse* are specified by the NIM standard.

- *Standard logic pulses*: Typically, these are of positive polarity, with widths on the order of a few  $\mu\text{s}$  and are used when the count rate is not excessive (dead time).
- *Fast logic pulses*: These are used primarily in fast timing circuits and for fast counting rates. They are usually of negative polarity with widths on the order of a few hundred nanoseconds. Since the timing marker is usually extracted from the leading edge, they tend to have very fast rise times (few nanoseconds). In order to avoid problems with reflections, fast pulses are usually handled in systems where all the impedances (input, output and cable) are matched and set to  $50\ \Omega$ .

## 3.2 STANDARDS FOR NUCLEAR INSTRUMENTATION: NIM AND CAMAC

Most commercially purchased instruments for nuclear measurement systems comply with either the NIM (Nuclear Instrument Module) or CAMAC (Computer Automated Measurement And Control) standard. Both of these are international standards that incorporate a wide range of mechanical and electrical definitions to facilitate cost and convenience advantages to the users.

Both NIM and CAMAC standards incorporate modular instruments that plug into a bin or crate and get their low-voltage power (usually  $\pm 6, 12, \text{ and } 24\ \text{V}$ ) from a standard power supply attached to the rear of the crate.

The CAMAC standard differs from NIM in two important ways.

i) The CAMAC crate has a built in digital data bus to provide computer communications with the modules and

ii) The narrowest CAMAC modules are exactly half the width of the minimum NIM module.

NIM standards for logic pulses are specified in Table 3.1.

<b>Table 3.1</b>		
NIM Standard Logic Levels		
	Output (must deliver)	Input (must respond to)
Logic `1'	+4 to +12V	+3 to +12V
Logic `0'	+1 to -2V	+1.5 to -2V
NIM Fast Logic Levels for 50 ohm System		
	Output (must deliver)	Input (must respond to)
Logic `1'	-14 to -18 mA	-12 to -36 mA
Logic `0'	-1 to +1 mA	-4 to +20 mA

### 3.3 PREAMPLIFIERS

#### 3.3.1 Matching the preamplifier to the detector and the application

The primary function of the preamplifier is to extract the signal from the detector without significantly degrading the intrinsic signal-to-noise ratio. Therefore, the preamplifier is usually located as close to the detector as possible to minimize the capacitive loading on the detector, and the input circuits of the preamp are designed to match the characteristics of the detector.

Several types of detector produce moderately large output pulses and this relaxes the restrictions that are placed on the preamplifier. Detectors that fall in this category include

- Photodiodes operating in intense light
- Photomultiplier tubes (PM tubes)
- Scintillation detectors mounted on a PM tube
- Microchannel plates
- Channeltrons and electron multipliers.

For such detectors, a wide-band amplifier with a low input impedance can often be used directly at the detector.

More care needs to be taken for high-resolution systems, such as those used for high-resolution X-ray,  $\gamma$ -ray or charged-particle spectroscopy. Typical detectors in this category include:

- Silicon (Si) detectors
- Germanium (Ge) detectors
- Gas proportional counters.

These detectors produce very small output signals. Therefore, it is important that the input stage of the preamp contributes very little noise. This requirement is often met by using a charge-sensitive preamplifier with a field-effect transistor (FET) input stage. To further reduce thermal noise, the FET is often cooled to near liquid-nitrogen temperatures (see Section 3.4).

### 3.3.2 Charge-sensitive preamplifiers

These are preferred for most spectroscopy applications. The signal from a semiconductor detector is a charge delivered as a current pulse lasting from  $10^{-5}$  to  $10^{-6}$  seconds depending on the type and size of the detector. For most applications, the parameters of interest are the total quantity of charge or the time of occurrence of the event or both. The charge-sensitive preamp, illustrated in Figure 3.1 can deliver both.

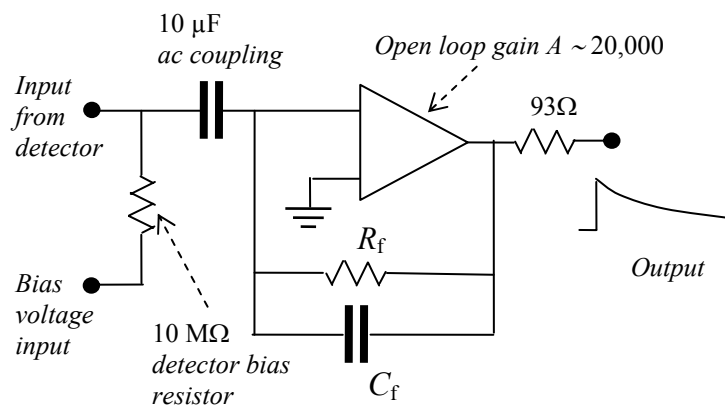


**Figure 3.1** Schematic diagram of an ac coupled charge-sensitive preamp.

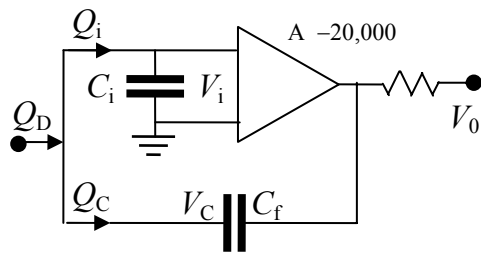
As long as the time constant on the feedback loop ( $R_f C_f$ ) is long compared to the duration of the input pulse, the output voltage is proportional to the total integrated charge in the pulse. The

output voltage from the preamp has an amplitude  $V_0$  and a decay time constant  $\tau_0$  given by

$$V_0 = Q_D/C_f \tag{3.1}$$

$$\text{and } \tau_0 = R_f C_f \tag{3.2}$$

where  $Q_D$  is the charge from the detector and  $C_f$  and  $R_f$  are the feedback capacitance and resistance respectively.



Derivation of Equation (3.1).  
 The diagram shows charges, voltages and essential elements in a charge-sensitive preamp  
 $V_0 = V_i + V_C$ , but  $A$  is large ( $\sim 20,000$ ), therefore,  
 $V_i = V_0/A \approx 0$  and so  $V_0 \approx V_C = Q_C/C_f$ .  
 Charge balance:  $Q_D = Q_C + Q_i$ , but  $Q_i = C_i V_i \approx 0$ .  
 Therefore,  $Q_D \approx Q_C$ , whence  
 $V_0 \approx Q_D/C_f$  independent of  $C_i$

The resistor  $R_f$  is a **noise source** and, in a dc coupled system, is kept as large as possible. The preamp package itself is made as small as possible and is mounted as close to the detector as practical to minimize noise from the input capacitance caused by cabling, ground loops, microphonics or radio-frequency pickup. All of these are sources of noise to a charge-sensitive preamp.

Noise in charge-sensitive preamps is generally controlled by four components:

- The input field-effect transistor (FET).
- The total capacitance of the input (detector capacitance, cables etc.).
- The resistance connected to the input.
- Input leakage currents from the detector and FET.

The FET is selected for low-noise performance and is often cooled to almost LN<sub>2</sub> temperature to reduce thermal noise.

The rise time of the voltage pulse at the output of the charge-sensitive preamp, in the ideal case, is equal to the charge collection time of the detector.

Electronic noise in a preamp is discussed in more detail in Section 3.4.

### 3.3.3 Preamp sensitivity

The performance of a preamp is normally given as output voltage per unit of energy deposited in a semiconductor detector, e.g. mV/MeV.

The charge delivered by a detector to its preamp is equal to

$$Q_D = \frac{Ee \times 10^6}{\varepsilon} \quad (3.3)$$

where  $E$  is the energy in MeV deposited in the detector,  $\varepsilon$  is the average energy in eV to produce an electron-hole (e-h) pair in the detector and  $e$  is the electronic charge ( $1.6 \times 10^{-19}$  C).

From Equation (3.1), the output voltage  $V_0 = Q_D/C_f = Ee \times 10^6 / \varepsilon C_f$  and, hence, the sensitivity  $V_0/E = e \times 10^6 / \varepsilon C_f$ .

**Example:** For  $C_f = 10^{-12}$  F and  $\varepsilon = 3.62$  eV/e-h (for a silicon detector)

$$\underline{V_0/E = 44 \text{ mV/MeV.}}$$

### 3.3.4 Current-sensitive preamplifier

Some detectors generate moderately large and fast rising output pulses (photomultiplier tubes, microchannel plates) with high output impedance. Pulse processing these signals for counting or timing can be less restrictive. A properly terminated 50 ohm cable attached to the detector output is sufficient (the current pulse develops the desired voltage across the load presented by the cable). For scintillators mounted on PM tubes, this voltage signal is usually large enough to drive a fast discriminator without additional amplification!

For smaller pulses (single-photon counting, etc), additional amplification is sometimes provided by the *current-sensitive preamplifier*, see Figure 3.2.

The 50-ohm input impedance is chosen to match the impedance of the cable and converts the current pulse to a voltage pulse. If the rise time of the preamp is negligible compared to that of the detector, then the amplitude of the voltage pulse is

$$V_{\text{out}} = 50 I_{\text{in}} A \quad (3.4)$$

where  $A$  is the gain of the preamp and  $I_{\text{in}}$  is the amplitude of the current pulse from the detector. For timing applications, this signal can drive the input of a counter/ratemeter etc.

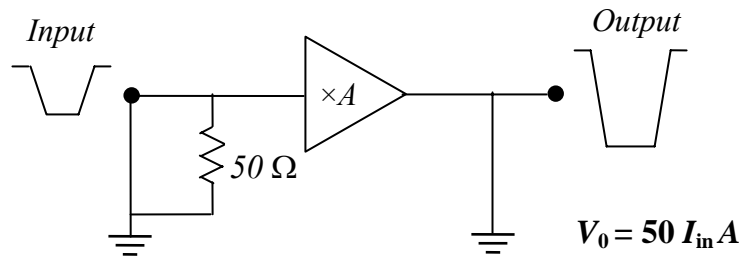


**Figure 3.2.** Schematic diagram of a current-sensitive preamplifier.

The dominant limitation on timing resolution with PM tubes arises from fluctuations in the transit time of the electrons cascading through the PM tube. This fluctuation causes a jitter in the arrival time of the pulse at the detector output. In addition, the effect of preamplifier input noise on the time resolution must also be considered. This noise will cause an uncertainty (jitter) in the time at which the pulse crosses the threshold in a timing discriminator, with a resulting deterioration in the time resolution of the system. To minimize this effect, choose a preamplifier with a rise time similar to or shorter than that of the detector. A preamplifier with a rise time much shorter than that of the detector output does not help. In fact, it is a source of additional noise because of the excessively large bandwidth (see Section 3.4).

### 3.3.5 Overload recovery and pile-Up

The overload recovery property is an important preamp specification for those applications where frequent large pulses might cause the system to saturate.

The output of a preamp is a tail pulse with a rather long decay time and, at any reasonable rate, pile-up of output pulses is inevitable. The effects of this pile-up are largely removed by subsequent pulse shaping but if the pile-up causes the system to **saturate**, then vital amplitude information is lost, see Figure 3.3. Reducing the value of the feedback resistance will help, but only at the expense of increased noise.

Another solution is to use an **automatic reset** in place of the resistive feedback. The feedback resistor is eliminated and the output voltage builds up (Figure 3.4) until a limit is reached. At that point the dc voltage is rapidly reset to zero volts after which the process repeats.

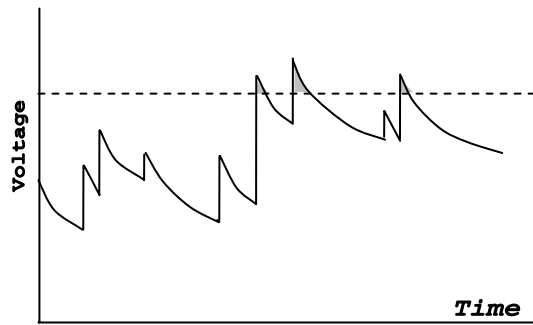


**Figure 3.3** Pile-up of preamp pulses at high rates.

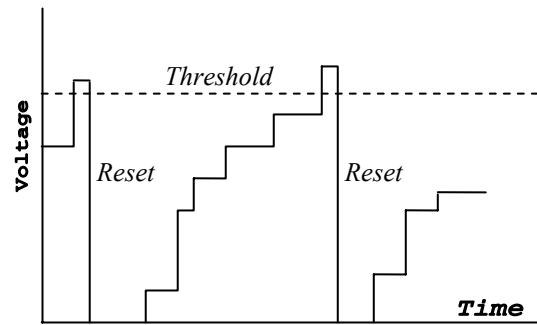


**Figure 3.4** Schematic representation of the voltages in an automatic reset preamplifier.

There are several ways of resetting the system:

- For low-energy X-ray systems, the reset is commonly performed by a **pulsed optical device** with an LED triggering a light-sensitive switch.
- For higher energies and/or at high rates, a **transistor reset** is used. These are referred to as transistor-reset preamplifiers.

The preamplifier is dead for a short time,  $T_{\text{reset}}$ , as it is being reset. This leads to an overall dead time, which is dependent on the count rate  $r$  and the average energy  $E$  per event. Specifically:

$$\% \text{ dead time} = 100 \left( \frac{E r T_{\text{reset}}}{E_{\text{reset}}} \right) \quad (3.5)$$

where  $E_{\text{reset}}$  is the reset threshold in units of deposited energy.

### 3.3.6 Detector bias voltage

The preamplifier is commonly used as a means of supplying the bias HV to the detector.

Figure 3.5 shows two possible configurations, ac and dc coupled, where the detector bias is applied through the resistance  $R_L$ . A single cable connects the preamplifier and the detector and provides both the signal to the preamp and HV to the detector. The load resistance  $R_L$ , together with the input capacitance determines the time constant across which the detector current is collected.

From the point of view of minimum noise contribution,  $R_L$  should be as large as possible (in



practice,  $R_L$  is seldom more than a few thousand  $M\Omega$  ).

Leakage currents drawn by the detector must flow through this resistance. Such leakage currents can be especially important for semiconductor detectors and in cases where  $R_L$  is large, can lead to a significant voltage drop across the resistor. In this case, the actual voltage seen by the detector is less than the supply voltage! Users must be aware of this so that the voltage dropped across  $R_L$  can be compensated for by raising the supply voltage.

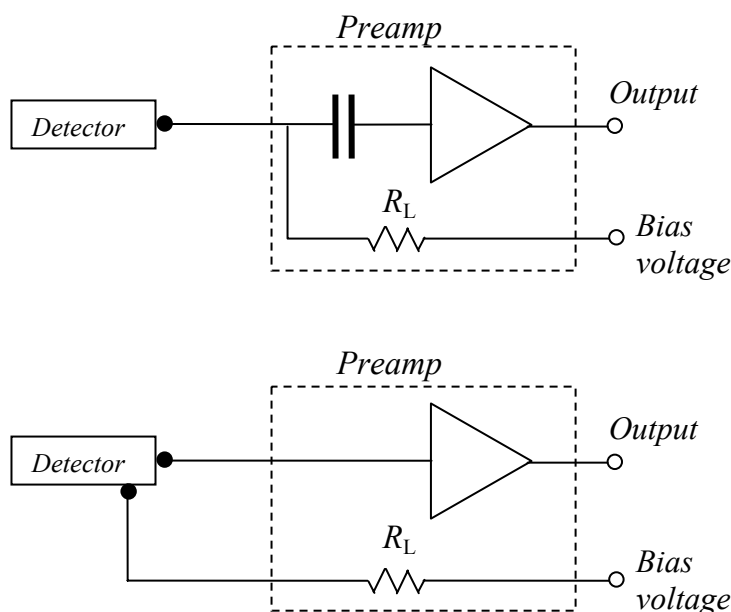


**Figure 3.5** Two possible configurations for supplying detector bias through the preamplifier.

The best noise performance usually results from the use of a FET (field-effect transistor) input stage in the preamplifier. FETs are notoriously sensitive to over-voltage transients and can easily be blown by voltage fluctuations generated when switching a detector on or off. For this reason, many (but not all) commercial preamplifier packages are provided with over-voltage protection (e.g. on Ge preamplifiers).

### 3.4 ELECTRONIC NOISE

Perhaps the most important specification for a preamplifier is its noise characteristics.

The noise figure is usually quoted as the FWHM of the response of the system due to only preamp noise and is given as the energy spread in the type of detector for which the preamplifier

was designed. The noise is obviously a strong function of the capacitance with which the preamp is loaded. This input capacitance arises both from the detector and the interconnecting cables.

For a wide variety of applications, the noise level of commercially available preamplifiers is low enough that their contribution is small compared to the inherent contribution of the detector itself. This is not always the case, for example, for low-energy measurements. Preamp noise is very important when measuring energy deposition in a semiconductor detector below a few keV.

Electronic noise is associated with the influence on an electronic signal of random statistical effects, such as thermal motion of charges in electronic components and the discrete nature of electric charge. Effects can be grouped into three main categories, which are distinguished by the different ways they respond to input parameters such as the amplifier shaping time constant. These categories are given the general names: **parallel noise**, **series noise** and **flicker noise**.

A full treatment of this subject is complex. These lecture notes, give a brief summary of the phenomena, including a short list of references for interested readers. Results are presented with highly simplified plausibility arguments in an attempt to justify the forms of the different expressions.

### 3.4.1 Parallel noise

Parallel noise is associated with currents flowing in components at the input to the preamplifier.

There are two main sources:

- Leakage current flowing through the detector and its circuitry. This is sometimes called **shot noise**.
- Thermal vibration of electrons in critical resistors, e.g. the preamplifier feedback resistor and the detector bias resistor. We shall refer to this as **thermal noise**. It is also called Johnson noise.

Each of these sources is treated as an **effective noise-current generator** at the input to the preamplifier.

*Shot noise:* In order to analyze this noise source we recognize that any current is a flow of discrete charge carriers, i.e. a series of discrete pulses of equal height arriving randomly in time. This is depicted in Figure 3.6.

Each pulse represents the passage of a single unit of charge  $e$  (an electron or hole). Mathematically, we can write this as  $e\delta(t)$ , where  $\delta(t)$  is the delta function. Its property is that it has a finite value only at time  $t$  and its integral over time is unity. Therefore, the integral of  $e\delta(t)$  over time is  $e$ , one unit of electronic charge.

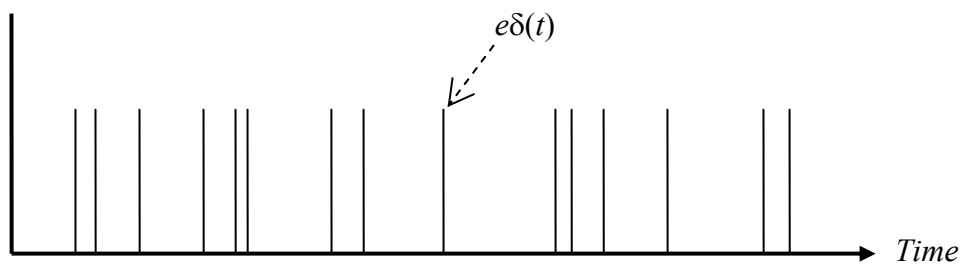


**Figure 3.6** A current represented as a train of pulses passing a given point randomly in time.

The leakage current is  $i_L = ne$ , where  $n$  is the average pulse rate, and if the amplifier shaping time constant is  $\tau$ , approximately  $N \approx n\tau$  pulses will have elapsed during the period of the signal pulse.

Thus, the average leakage charge collected in this period is  $Q_{av} = Ne$ .

Since the pulses arrive randomly in time, the number  $N$  is subject to Poisson statistics, i.e. the number  $N$  has a standard deviation of  $\sqrt{N}$  and a relative standard deviation of  $1/\sqrt{N}$ . Therefore, the actual charge collected in time  $\tau$  will exhibit a statistical variation, which is observed as noise on the signal.

Noise is quoted as the **variance** (standard deviation squared) of the collected charge. Thus, we can write shot (leakage current) noise as

$$(\omega)_{\text{shot}}^2 = (Q_{av} / \sqrt{N})^2 = Ne^2$$

which can be written as

$$(\omega)_{\text{shot}}^2 = ne^2 \tau = ei_L \tau. \quad (3.6)$$

using the above expressions for  $i_L$  and  $N$ .

Note that the units are (charge)<sup>2</sup>.

**Example:** We use the above general arguments and our knowledge of detectors to estimate the effect of shot noise on the signal from a germanium detector.

- Suppose the detector leakage current is 1 nA. This is equivalent to a flow rate  $n \sim 6 \times 10^9$  electrons per second.
- If we have set a shaping time constant  $\tau$  of 6  $\mu\text{s}$ ,  $N = n\tau \sim 4 \times 10^4$  and  $\sqrt{N} \sim 200$ .
- In a germanium detector, about 3 eV is required to create an electron-hole pair. So, a variation of 200 charge carriers is equivalent to **600 eV** of noise on the energy signal.

*Thermal noise:* As we have already indicated, this noise source arises from the thermal motion of charge carriers in a resistor, the most important being the preamplifier feedback resistor  $R$ .

- The motion is driven by thermal energy  $kT$  where  $k$  is Boltzmann's constant and  $T$  is the absolute temperature.
- We can consider that there is a varying effective voltage  $V$  across the resistor, where  $eV = kT$  is the thermal energy of an electron in the resistor.
- This voltage generates a (thermal) current  $i_{\text{th}} = V/R$ .
- This current can be treated as an **effective input source** and, following an analysis similar to that given above for shot noise [Equation (3.6)], we find a thermal noise variance

$$(\omega)_{\text{th}}^2 \approx e i_{\text{th}} \tau = \left( \frac{eV}{R} \right) \tau = \left( \frac{kT}{R} \right) \tau$$

after substituting for  $i_{\text{th}}$  and  $eV$ .

A proper calculation gives

$$(\omega)_{\text{th}}^2 \approx \left( \frac{4kT}{R} \right) \tau . \quad (3.7)$$

Shot noise and thermal noise contribute to parallel noise and we add the variances:

$$(\omega)_{\text{parallel}}^2 \approx e i_{\text{L}} \tau + \left( \frac{4kT}{R} \right) \tau . \quad (3.8)$$

Note that both terms have the same dependence on the shaping time constant  $\tau$ .

Parallel noise is minimized by

- Reducing  $T$  (cooling the feedback and bias resistors).

- Using a large feedback resistor (or an autotest preamplifier).
- Using a short shaping time constant  $\tau$ .

### 3.4.2 Series noise

This noise source is due to leakage current  $i_D$  in the preamplifier field-effect transistor (FET). It has a completely different dependence on shaping time to that of shot noise or thermal noise. This is because  $i_D$  is a property of the transistor (and its temperature) and is not dependent on the shaping time  $\tau$ .

Consider  $i_D$  to be due to electrons flowing at a rate  $n$  per unit time, i.e.

$$i_D = ne. \quad (3.9)$$

During the shaping time  $\tau$ , a number  $N = n\tau$  electrons will have been collected. The standard deviation of this number is  $\sqrt{N}$  and so  $i_D$  and, hence, the output will fluctuate because of it:

$$i_D = ne = Ne/\tau \pm \sqrt{N}e/\tau = ne \pm \sqrt{ne}/\sqrt{\tau}.$$

Thus, we see that the variance (standard deviation)<sup>2</sup> of the FET current is proportional to  $ne^2/\tau$ . The output voltage due to FET leakage is proportional to  $i_D$  and so the variance in the output (series noise) will also vary as  $1/\tau$  and not directly with  $\tau$  as we found with parallel noise. Thus we have

$$(\omega)_{\text{series}}^2 \propto ne^2/\tau. \quad (3.10)$$

Series noise depends on other parameters. In particular, it depends on **temperature** because FET leakage depends on temperature. It also depends on **input capacity**  $C_i$  and FET **transconductance**  $g$ .

We use a crude plausibility argument to gain some insight into the origin of these dependences. This is done by calculating the FET noise current  $i_D$  as if it were due to an **effective noise source**  $i_S$  at the **input** to the preamplifier. This procedure also enables us to relate FET leakage noise (series noise) with detector shot noise and thermal noise (parallel noise).

An equivalent circuit, showing the essential components needed for our analysis, is presented in Figure 3.7.

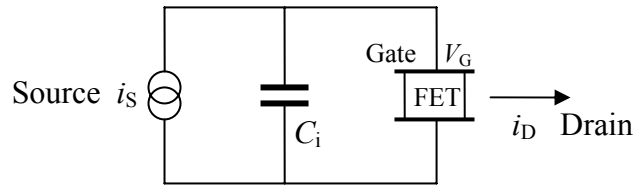


**Figure 3.7** Schematic equivalent circuit, showing an input source  $i_S$ , which generates an FET drain current  $i_D$ .

A pulse at the input can be represented as  $i(t) = e\delta(t)$ , where  $\delta(t)$  is the delta function. This pulse contains an amount of charge  $e$ , and it generates a voltage increment  $\Delta V_G = e/C_i$  at the FET gate, where  $C_i$  is the input capacitance.

The transconductance of a transistor is defined as

$$g = \partial i_D / \partial V_G. \quad (3.11)$$

Thus, the voltage increment  $\Delta V_G$  at the FET input generates an FET drain current  $\Delta i_D = g\Delta V_G = ge/C_i$ .

It follows from this that an increment in FET drain current,  $\Delta i_D = e$ , would result from an amount of charge  $C_i e/g$ , from an effective input source, collected on  $C_i$ .

Hence, we can obtain an approximate expression for  $(\omega)_{\text{series}}^2$  by considering the noise to arise from effective shot noise at the input to the preamp and replacing  $e$  in the Equation (3.10) with  $C_i e/g$ . i.e.

$$(\omega)_{\text{series}}^2 \propto \left( \frac{C_i}{g} \right)^2 \frac{e^2 n}{\tau}. \quad (3.12)$$

The temperature dependence is contained in the quantity  $n$ , and is obtained from an approximate relationship between transistor drain current  $i_D$  and gate voltage  $V_G$ :

$$i_D \approx e^{eV_G/kT} \quad (3.13)$$

as is illustrated in Figure 3.8.

Differentiating Equation (3.13) gives  $\partial i_D / \partial V_G = (e/kT)i_D$ , which can be written as  $g = (e^2 n/kT)$ , using Equations (3.9) and (3.11). Then, substituting for  $e^2 n$  in Equation (3.12) gives

$$(\omega)_{\text{series}}^2 \propto \left(\frac{C_i}{g}\right)^2 \frac{gkT}{\tau} = C_i^2 \left(\frac{kT}{g\tau}\right). \quad (3.14)$$

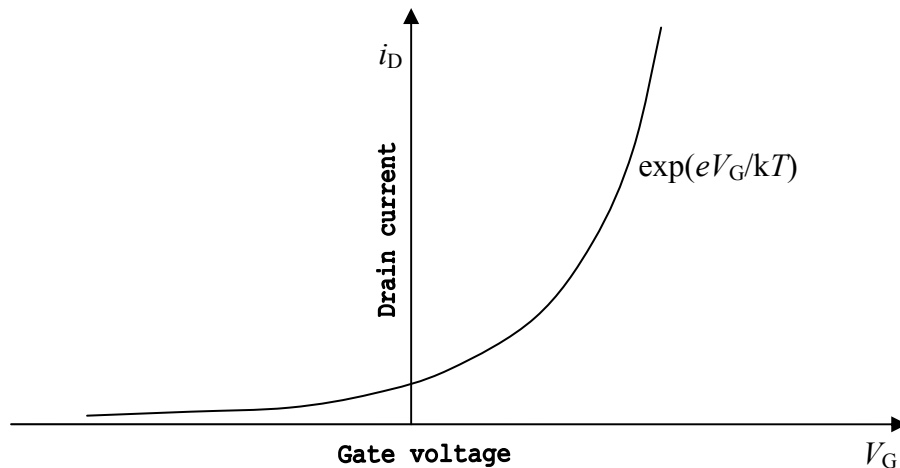


**Figure 3.8** Variation of drain current  $i_D$  with gate voltage  $V_G$  in a FET.

We stress that the above is not a proper derivation of series noise. However, apart from numerical constants, Equation (3.14) is the form of the expression for series noise given by a more rigorous calculation.

Series noise is minimized by

- Reducing the input impedance  $C_i$  (length of connecting leads etc.).
- Lowering the temperature (cooling the FET and feedback resistor).
- Using a high gain ( $g$ ), low-noise FET.
- Increasing the shaping time.

### 3.4.3 Flicker noise

We note that there is a third noise source, flicker noise, which is not dependent on the shaping time. It arises from currents in all active components and increases with count rate. However, it is generally much smaller than either parallel or series noise and we do not attempt to analyze it here.

### 3.4.4 Noise and amplifier shaping time.

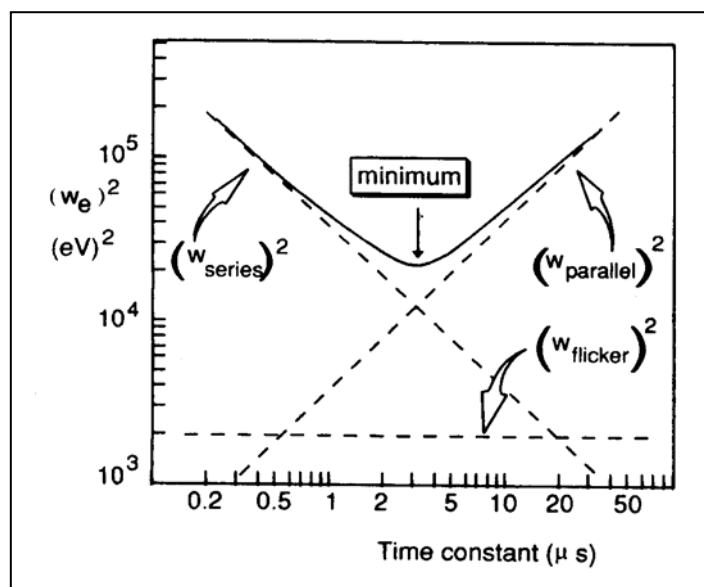


**Figure 3.9** Impressionistic diagram showing how addition of various noise contributions leads to a minimum in the total noise at a particular time constant.

Figure 3.9 shows the three noise contributions plotted as functions of the shaping time constant  $\tau$  in  $\mu\text{s}$ .  $(\omega)_{series}^2$  decreases with  $\tau$  and  $(\omega)_{parallel}^2$  increases with  $\tau$ , so, in general, there will be an optimum value of  $\tau$  which achieves a minimum in the total electronic noise level.

In any given situation, the plots will depend on the particular detector and electronics used. For example, parallel noise can be reduced by using an auto-reset preamplifier because there is no feedback resistor. Reducing  $(\omega)_{parallel}^2$  will shift the minimum to a longer time constant. However, a long time constant is not desirable if the counting rate is very high and a different compromise may have to be reached.

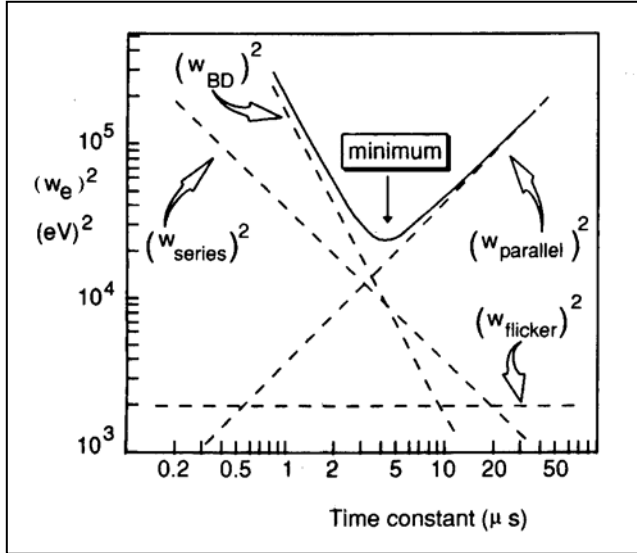
### 3.4.5 Ballistic deficit

Figure 3.10 illustrates a situation where there is a noise contribution  $(\omega)_{BD}^2$  arising from ballistic deficit in the signal when the collection time of charges liberated in the detector is not short compared with the shaping time constant. The contribution  $(\omega)_{BD}^2$  is shown to vary inversely with the square of the time constant and, if it is more important than  $(\omega)_{series}^2$ , the minimum in the variation of total noise vs time constant will be skewed and not symmetric as it



is in Figure 3.9.

Conversely, we might say that if the noise curve is measured and found to be skewed, it suggests that ballistic deficit may be significant and limiting the system resolution.



**Figure 3.10** Impressionistic diagram of electronic noise contributions with a significant ballistic-deficit contribution.

### 3.5 A PRACTICAL EXAMPLE

In the previous section, we have considered various sources of electronic noise and how they might affect the energy resolution of a signal from a radiation detector. Note that energy resolution is proportional to the fluctuation or standard deviation of repeated measurements of the energy signal. Since the various sources of noise are independent of each other, their contributions must be added in quadrature to obtain the total electronic noise. This is why it is the noise variances that are calculated and are added together. The energy resolution is the square

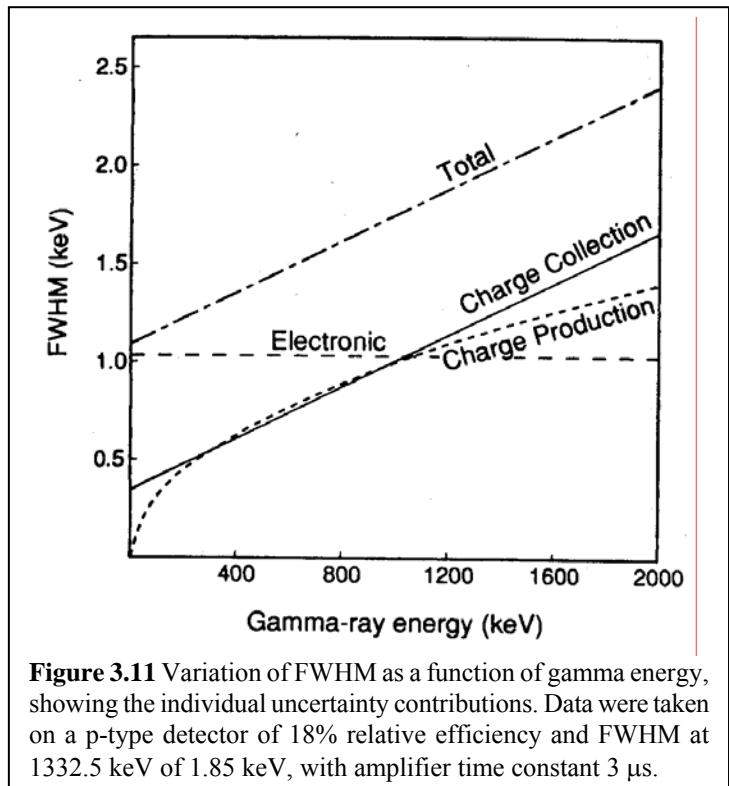


**Figure 3.11** Variation of FWHM as a function of gamma energy, showing the individual uncertainty contributions. Data were taken on a p-type detector of 18% relative efficiency and FWHM at 1332.5 keV of 1.85 keV, with amplifier time constant 3 μs.

root of the sum of the variances of all the contributions.

Other sources of fluctuations in the energy signal arise from the statistics of charge production and variation in charge collection efficiency in the detector.

The statistics of **charge production** is proportional to the square root of the number of electron/hole pairs produced by the radiation, which is proportional to the radiation energy  $E_\gamma$ . Thus, the energy resolution (FWHM) due to this source will be proportional to  $\sqrt{E_\gamma}$ , whereas **electronic noise**, discussed above, is independent of  $E_\gamma$ . Both these contributions are plotted in Figure 3.11, which is a practical example of a real situation.

- The total measured resolution, as a function of  $E_\gamma$ , is shown as the dot-dashed curve.
- The line labelled 'Charge Collection' was obtained from the measured 'Total' by subtracting the 'Electronic' and 'Charge production' contributions in quadrature.
- At low energy, the noise is mainly electronic, whereas higher energies show an increasing importance of charge production and particularly of charge collection, which eventually is the dominant source.

Note that incomplete charge collection in a detector generally manifests as a low-energy tail on the total-energy peak in the spectrum. Such a tail suggests either that the detector bias is too low or that the detector is radiation damaged and has regions where the charges become trapped and are unavailable to be collected. The charge collection time can be affected in such situations and this can lead to ballistic-deficit effects, an indication of which is a skewed curve of noise versus shaping time, as described above. In such a situation, the use of a gated integrator should be considered (see Lecture 2).

### 3.6 REFERENCES

The following have some treatment of noise in detectors and electronic components and are roughly in order of increasing complexity.

Knoll, G F. (2000) *Radiation Detection and Measurement*, 3<sup>rd</sup> edition, John Wiley, New York.

EG&G Ortec (1991/92), *Detectors and Instruments for Nuclear Spectroscopy*, EG&G Ortec, Oak Ridge, USA.

Canberra Reference 1, (1991), *Detector Basics*, 2<sup>nd</sup> edition, Canberra Semiconductor NV, Olen, Belgium.

Dowding, B. (1988), *Principles of Electronics*, Prentice Hall, New York.

Nicholson, P. W. (1974), *Nuclear Electronics*, John Wiley, New York.

Radeka, V. (1988), Low Noise Techniques in Detectors, *Annual Review of Nuclear and Particle Science*, **38**, 217 - 277.